Anisotropy in collective precessional dynamics in arrays of $Ni_{80}Fe_{20}$ nanoelements

B. Rana, D. Kumar, S. Barman, S. Pal, R. Mandal, Y. Fukuma, Y. Otani, S. Sugimoto, and A. Barman

Citation: Journal of Applied Physics **111**, 07D503 (2012);
View online: https://doi.org/10.1063/1.3672402
View Table of Contents: http://aip.scitation.org/toc/jap/111/7
Published by the American Institute of Physics

Anisotropy in collective precessional dynamics in arrays of $Ni_{80}Fe_{20}$ nanoelements

B. Rana,[1] D. Kumar,[1] S. Barman,[1] S. Pal,[1] R. Mandal,[1] Y. Fukuma,[2] Y. Otani,[2,3] S. Sugimoto,[3] and A. Barman[1,a)]

[1]*Department of Condensed Matter Physics and Material Sciences, S. N. Bose National Centre for Basic Sciences, Block JD, Sector III, Salt Lake, Kolkata 700 098, India*
[2]*Advanced Science Institute, RIKEN, 2-1 Hirosawa, Wako, Saitama 351-0198, Japan*
[3]*Institute for Solid State Physics, University of Tokyo, 5-1-5 Kashiwanoha, Kashiwa, Chiba 277-8581, Japan*

(Presented 31 October 2011; received 23 September 2011; accepted 26 October 2011; published online 23 February 2012)

The anisotropy in the collective precessional dynamics with the variation of azimuthal angle of the bias magnetic field is studied in arrays of permalloy ($Ni_{80}Fe_{20}$) nanoelements by an all-optical time-resolved Kerr microscope. When the nanoelements are very closely spaced (inter-element separation = 50 nm), a gradual transition from completely uniform collective regime to a completely non-collective regime is observed as the azimuthal angle varies from 0° to 45°. On the other hand, for inter-element separation of 100 nm, a non-uniform collective dynamics is observed at 0° and a non-collective dynamics is observed at 45° but no clear trend in the transition is observed. © *2012 American Institute of Physics*. [doi:10.1063/1.3672402]

Ordered arrays of magnetic nanoelements have emerged as a topic of scientific and technological interests due to the richness of the magnetization reversal dynamics[1,2] and spin wave modes and damping in such systems,[3–10] as well as the potential technological interests. The later includes the devices including magnetic storage,[11] memory,[12] logic,[13] magnonic crystals[14] and arrays of spin torque nano oscillators.[15] Experimental and theoretical studies of magnetization precession in ordered arrays of nanomagnets have revealed various interesting observations including the size dependent precession frequency and damping, collective modes, anisotropic spin wave propagation, dynamic configurational anisotropy and observations of rich spin wave mode structures.[3–10]

The collective dynamics is determined by the interplay between the static and dynamic stray fields and with the variation of the relative orientation of the bias field both the internal fields within the individual elements and the stray fields are expected to vary and result in the variation in the collective mode structures. However, very few attempts have been made to study the dependence of collective modes on the relative orientation of the applied bias field and the symmetry of the array.[7] Here, we present the precessional dynamics of square arrays of square magnetic elements, where the individual elements possess non-uniform ground states and consequently a number of resonant modes are observed as the bias field direction is varied from the edge to the diagonal of the elements. We investigate how the anisotropy in the spin wave manifold is affected by the strength of the magnetostatic coupling as the arrays undergo transition from a single uniform collective mode to a number of non-uniform collective modes.

The samples were prepared by a combination of electron beam evaporation and electron-beam lithography. We investigated arrays of square permalloy elements of 200 nm width, 20 nm thickness and with edge to edge inter-element separation (S) of 50 nm and 100 nm. The scanning electron micrographs (Fig. 1(a)) show that the dots are of very good quality. The ultrafast magnetization dynamics of the arrays were studied by a home built all-optical time-resolved magneto-optical Kerr effect microscope.[16,17] About 8 mW of 400 nm laser pulses (pulse width ∼100 fs) were used to pump the samples while 2 mW of 800 nm laser pulses (pulse width ∼70 fs) were used to probe the dynamics. The bias field was tilted at 15° angle from the plane of the sample. The azimuthal angle (ϕ) of the in-plane component of bias field ($\boldsymbol{H}$) is varied and the time-resolved signals were measured at each ϕ value. The precessional dynamics appears as an oscillatory signal above the slowly decaying part of the time-resolved Kerr rotation signal after a fast demagnetization within 500 fs, and a fast remagnetization within 10 ps.

Figure 1(b) shows the bi-exponential background subtracted time-resolved Kerr rotations and the corresponding fast Fourier transform (FFT) spectra from the array with $S = 50$ nm at some selected values of ϕ for $H = 1.25$ kOe. For $\phi = 0°$, 90° and 180°, we observe a single uniform collective mode of the elements but at intermediate values of ϕ, we observe a splitting of the single mode into two modes. The frequencies of the modes vary significantly with ϕ. In Fig. 1(c), we have plotted the central frequency of each resonance peak as a function of ϕ. Two well separated branches are visible, where the upper branch is observed for all values of ϕ, whereas the lower branch is missing along three symmetry axes ($\phi = 0°$, 90° and 180°). A clear four-fold anisotropy is observed in the angular variation of the frequency for both branches with the easy axes at $\phi = 45°$ and 135° and hard axes at $\phi = 0°$, 90°, and 180°. The angular variation of frequency is fitted with Kittel's formula after introducing a four-fold anisotropy constant K_4 and assuming zero magnetocrystalline anisotropy for permalloy[18]

a)Author to whom correspondence should be addressed. Electronic mail: abarman@bose.res.in.

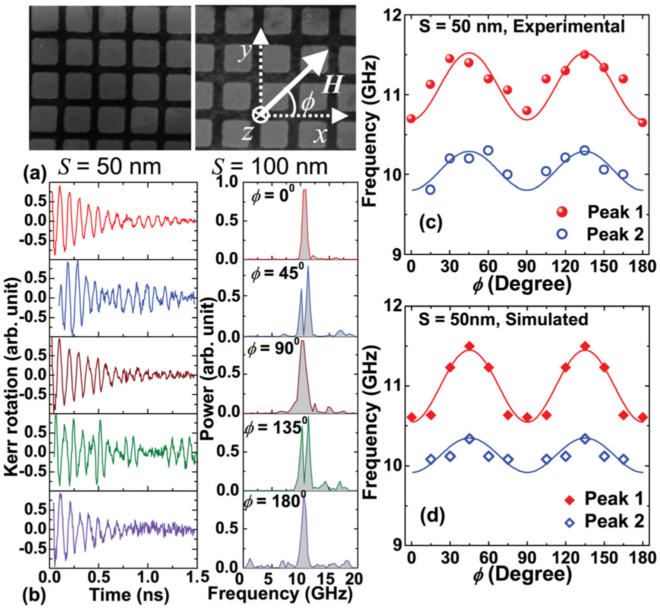

FIG. 1. (Color online) (a) Scanning electron micrographs of arrays of permalloy square elements with width = 200 nm, thickness = 20 nm and with varying inter-element separation S. The experimental geometry is shown on top of the image. (b) Experimental time resolved Kerr rotations and corresponding FFT spectra are shown for arrays of permalloy elements with $S = 50$ nm for varying angle of applied bias field (ϕ). (c) The experimental and (d) the simulated precession frequencies are plotted as a function of the angle (ϕ) of applied bias field. The solid lines correspond to fit to Eq. (1).

$$f = \frac{\gamma}{2\pi}\sqrt{\left[H - \frac{4K_4}{M}\cos 4\phi\right]\left[H + 4\pi M - \frac{K_4}{M}(3 + \cos 4\phi)\right]}, \tag{1}$$

where γ is the gyromagnetic ratio and M is the effective magnetization of the sample within the region where the mode occurs. The upper and lower branches show four-fold anisotropy fields (K_4/M) of about 22 Oe and 14 Oe, respectively.

We have further performed micromagnetic simulations by using OOMMF software[19] on arrays of 7×7 square permalloy elements with similar dimensions as the experimental samples and by dividing the samples into cuboidal cells of $5 \times 5 \times 20$ nm^3 volume. The bias field was applied in experimental configurations and a pulsed excitation was given along z directions for the dynamic simulations.[20] The simulated mode frequencies are plotted as a function of ϕ in Fig. 1(d), which reproduces the key experimental observations with the four-fold anisotropy fields (K_4/M) of 25 Oe and 13 Oe for the upper and lower branches, respectively.

We have also simulated the angle variation of the magnetization dynamics of a single 200 nm^2 permalloy element. Figure 2(a) shows the plot of mode frequencies as a function of ϕ. Four distinct branches are observed, out of which branches 2 and 4 show four-fold anisotropy with anisotropy fields (K_4/M) of 16 Oe and 8 Oe, respectively, while the other two branches show no clear symmetry. At $\phi = 0°$, 90°, and 180° two well separated modes are observed, out of which the lower frequency mode is clearly suppressed in the array with $S = 50$ nm. At 45° and 135° two modes are again observed. At intermediate values of ϕ, we observe four

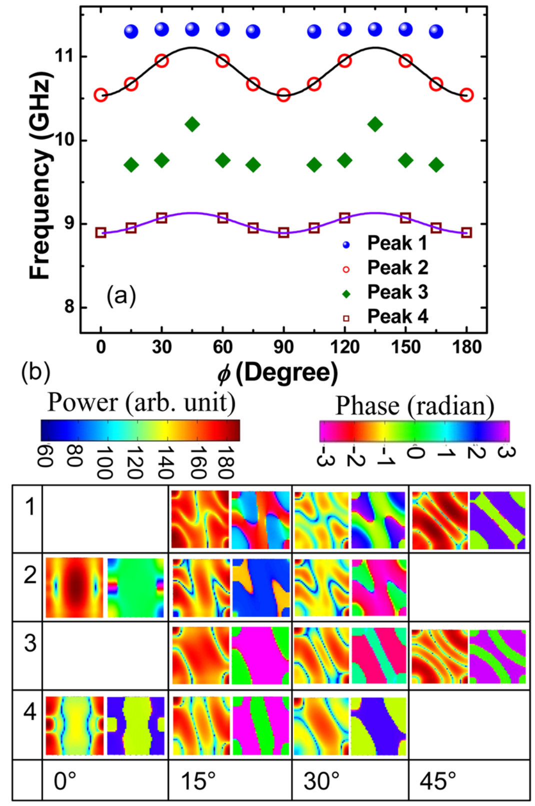

FIG. 2. (Color online) (a) Simulated precession frequencies as a function of the angle (ϕ) of the applied bias field and fit to Eq. (1) (solid lines) are shown for a single square permalloy element with width 200 nm and thickness 20 nm. (b) The powers and phases of the resonant modes are shown. The peak numbers are shown in the first column whereas ϕ is shown at the fifth row.

modes for the single elements but in the arrays two of those modes disappear, while two other modes are modified.

We have further simulated the power and phase maps of each resonant mode for both the single 200 nm element (Fig. 2(b)) and for the array with $S = 50$ nm (Fig. 3). We concentrated on the 3×3 elements at the center of the array,

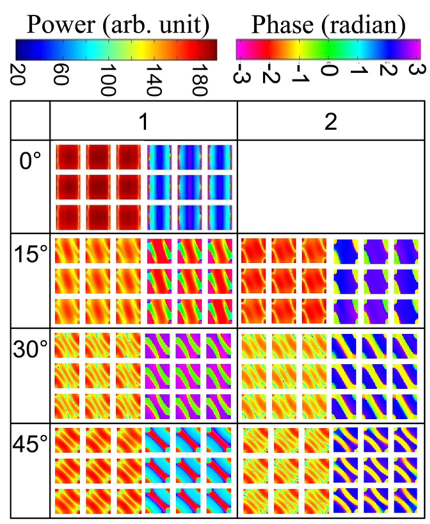

FIG. 3. (Color online) The powers and phases of the resonant modes for the arrays of square permalloy elements with $S = 50$ nm and with different bias field orientations (ϕ) are shown. The peak numbers are shown in the first row whereas ϕ is shown at the first column.

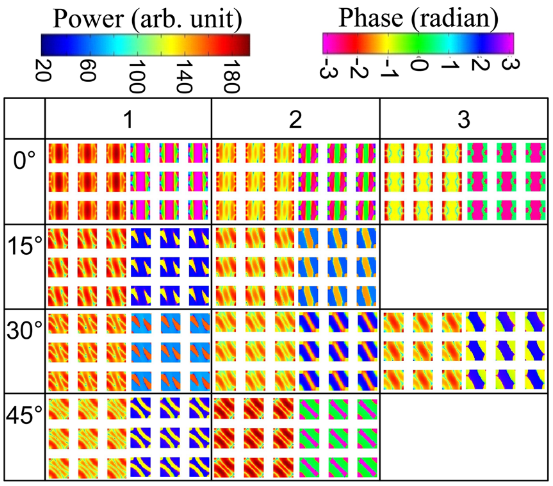

FIG. 4. (Color online) The powers and phases of the resonant modes for the arrays of square permalloy elements with $S = 100$ nm are shown at different values of ϕ. The peak numbers are shown in the first row whereas ϕ is shown in the first column.

which experience almost uniform magnetostatic environment. At $\phi = 0°$, the two modes are the center and edge modes of the single element and clearly the edge mode is suppressed in this array due to the strong magnetostatic fields from the neighboring elements. When the bias field is applied along directions between two edges of the elements a mixture of backward volume magnetostatic (BWVMS) and magnetostatic surface wave (MSSW) modes with different mode numbers (mixed modes) are observed. At the intermediate angles (15° and 30°), modes 1 and 4 are completely suppressed, while modes 2 and 3 are modified due to the inter-element interaction in the array. However for $\phi = 45°$, both the modes remain intact with slight modification in their frequencies. Hence, the collective dynamics is almost non-existent for $\phi = 45°$ although it appears to varying extent for $0° \leq \phi < 45°$ in arrays with $S = 50$ nm.

We further investigate the array with $S = 100$ nm. Figure 4 shows three modes at $\phi = 0°$, which are the center and edge modes of the individual elements, and an additional BWVMS like collective mode of the array. However, at $\phi = 15°$ two mixed modes are observed. For $\phi = 30°$ three mixed modes are observed, while for $\phi = 45°$ again two mixed modes (identical to the single element) are observed. The edge mode is absent for $\phi = 15°$, 30°, and 45°. Although, there is a common observation of non-collective dynamics at $\phi = 45°$ for both $S = 50$ nm and 100 nm, in the former case the transition from strongly collective regime ($\phi = 0°$) to non-collective regime ($\phi = 45°$) occurs gradually, while in the latter case no clear trend is observed.

In summary we have studied the dependence of the azimuthal angle (ϕ) of the bias field on the collective modes in arrays of permalloy elements with 200 nm width, 20 nm thickness and with inter-element separations (S) of 50 nm and 100 nm. Measurements and simulations show a uniform collective mode for $S = 50$ nm and transition to a non-uniform collective regime at $S = 100$ nm with the splitting of the main resonant mode. For $S = 50$ nm, a gradual transition from uniform collective regime to a non-collective regime occurs as ϕ changes from 0° to 45°. On the other hand, in the weakly collective regime ($S = 100$ nm) although the dynamics at $\phi = 45°$ is non-collective similar to that for $S = 50$ nm, transition from 0° to 45° does not follow a clear pattern.

We gratefully acknowledge the financial supports from Department of Science and Technology, Government of India under the grant numbers SR/NM/NS-09/2007, INT/EC/CMS (24/233552), FTP/PS-71/2007 and INT/JP/JST/P-23/09, and Japan Science and Technology Agency Strategic International Cooperative Program under the grant number 09158876.

[1]M. Hwang, M. C. Abraham, T. A. Savas, H. I. Smith, R. J. Ram, and C. A. Ross, J. Appl. Phys. **87**, 5108 (2000).
[2]L. J. Heyderman, H. H. Solak, C. David, D. Atkinson, R. P. Cowburn, and F. Nolting, Appl. Phys. Lett. **85**, 4989 (2004).
[3]S. Jung, B. Watkins, L. DeLong, J. B. Ketterson, and V. Chandrasekhar, Phys. Rev. B **66**, 132401 (2002).
[4]V. V. Kruglyak, A. Barman, R. J. Hicken, J. R. Childress, and J. A. Katine, Phys. Rev. B **71**, 220409 (2005).
[5]G. Gubbiotti, M. Madami, S. Tacchi, G. Carlotti, and T. Okuno, J. Appl. Phys. **99**, 08C701 (2006).
[6]Z. K. Wang, H. S. Lim, V. L. Zhang, J. L. Goh, S. C. Ng, M. H. Kuok, H. L. Su, and S. L. Tang, Nano Lett. **6**, 1083 (2006).
[7]V. V. Kruglyak, P. S. Keatley, R. J. Hicken, J. R. Childress, and J. A. Katine, Phys. Rev. B **75**, 024407 (2007).
[8]A. Barman and S. Barman, Phys. Rev. B **79**, 144415 (2009).
[9]V. V. Kruglyak, P. S. Keatley, A. Neudert, R. J. Hicken, J. R. Childress, and J. A. Katine, Phys. Rev. Lett. **104**, 027201 (2010).
[10]S. Tacchi, M. Madami, G. Gubbiotti, G. Carlotti, H. Tanigawa, T. Ono, and M. P. Kostylev, Phys. Rev. B **82**, 024401 (2010).
[11]O. Hellwig, A. Berger, T. Thomson, E. Dobisz, Z. Bandic, H. Yang, D. Kercher, and E. E. Fullerton, Appl. Phys. Lett. **90**, 162516 (2007).
[12]S. Tehrani, E. Chen, M. Durlam, M. DeHerrera, J. M. Slaughter, J. Shi, and G. Kerszykowski, J. Appl. Phys. **85**, 5822 (1999).
[13]A. Imre, G. Csaba, L. Ji, A. Orlov, G. H. Bernstein, and W. Porod, Science **311**, 205 (2006).
[14]S. Neusser and D. Grundler, Adv. Mater. **21**, 2927 (2009); A. V. Chumak, V. S. Tiberkevich, A. D. Karenowska, A. A. Serga, J. F. Gregg, A. N. Slavin, and B. Hillebrands, Nat. Commun. **1**, 141 (2010).
[15]S. Kaka, M. R. Pufall, W. H. Rippard, T. J. Silva, S. E. Russek, and J. A. Katine, Nature **437**, 389 (2005).
[16]S. Pal, B. Rana, O. Hellwig, T. Thomson, and A. Barman, Appl. Phys. Lett. **98**, 082501 (2011).
[17]B. Rana, S. Pal, S. Barman, Y. Fukuma, Y. Otani and A. Barman, Appl. Phys. Expr. 4, 113003 (2011).
[18]A. Barman, V. V. Kruglyak, R. J. Hicken, A. Kundrotaite, and M. Rahman, Appl. Phys. Lett. **82**, 3065 (2003).
[19]M. Donahue and D. G. Porter, OOMMF User's guide, Version 1.0, Interagency Report NISTIR **6376**, National Institute of Standard and Technology, Gaithersburg, MD (1999). Available at http://math.nist.gov/oommf.
[20]A. Barman and R. C. Sharma, J. Appl. Phys. **102**, 053912 (2007).